Scanning TEM (STEM): Imaging & Resolution

Duncan Alexander
EPFL-CIME

Contents

Principles of STEM

e⁻-matter interactions

- With STEM we can use many more of these signals in a highly spatially-resolved way than we can with TEM
- Furthermore we can record different signals in parallel, have an improved ultimate resolution and more easily interpretable atomic resolution images

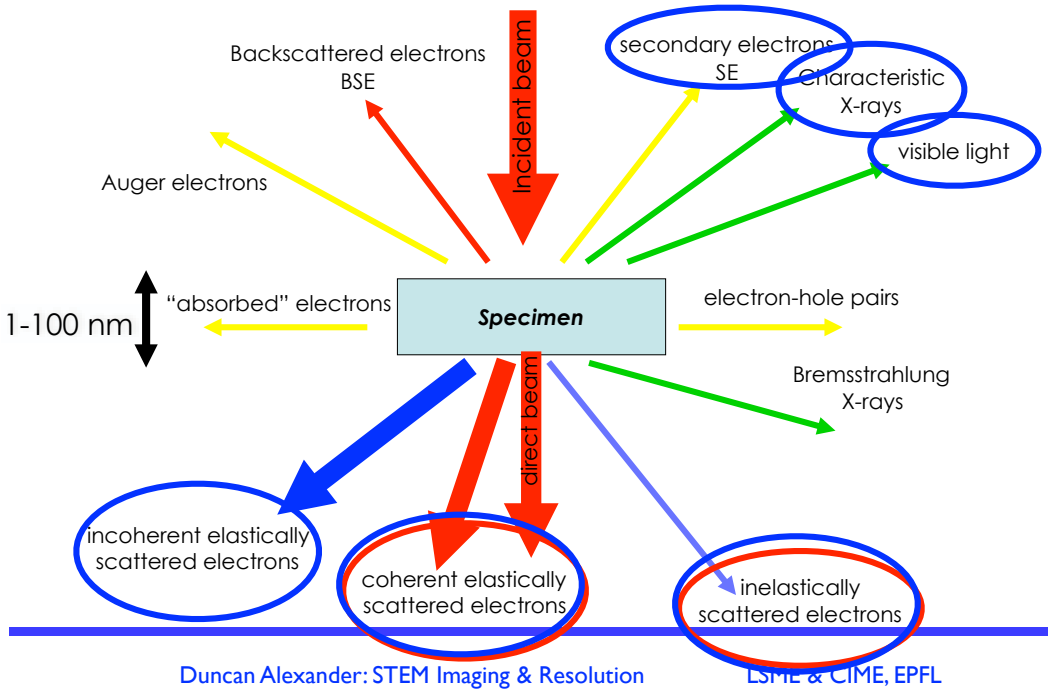

Principle of STEM

- Electromagnetic lens focuses electrons from FEG on to sample
- Beam deflectors scan beam across sample
- For each probe position (x, y) record signal intensity $I(x, y)$ and/or spectrum
  - Display/record image(s) of $I(x, y)$
  - Integrated signal from hyperspectral datasets (e.g. 3D datacube axes x, y, E)

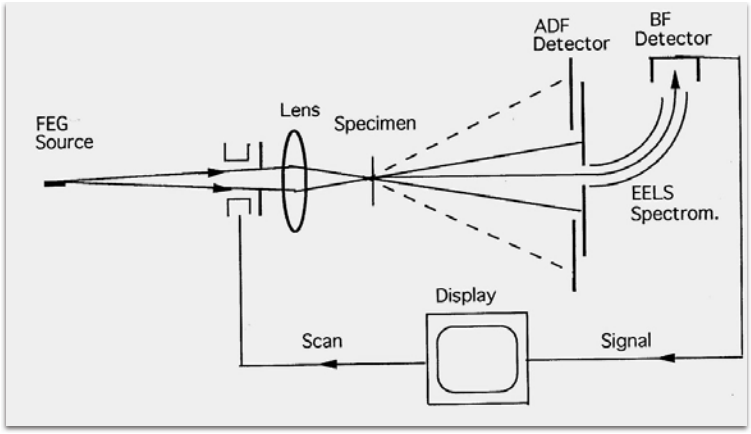

Optics of TEM vs STEM

- TEM: fixed beam, broad "parallel" illumination, objective lens that forms image after the specimen. Image projected onto camera
- Scanning TEM: lens forms focused probe on sample, scanned across sample in raster pattern. For each probe position (x, y) detect a signal intensity (or spectrum), convert to (x, y) image.

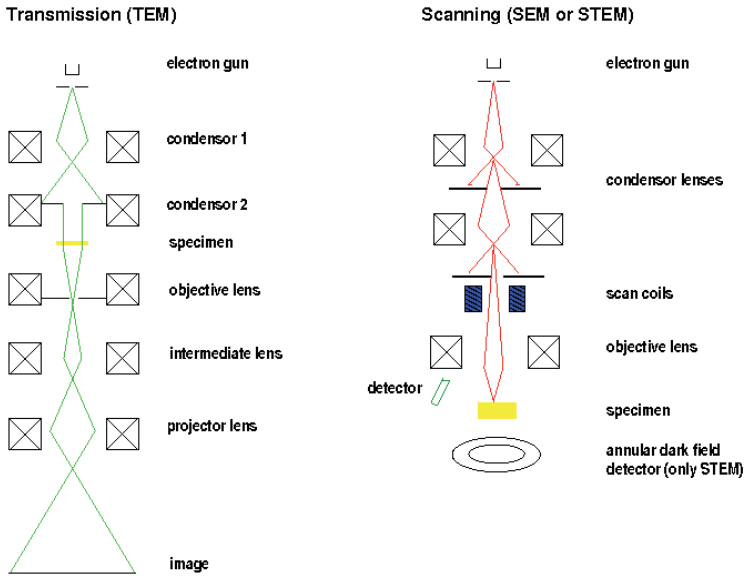

Quiz: what type of diffraction pattern will one see in STEM mode?

Convergent beam electron diffraction

Diffraction with a convergent beam (CBED)
Exact two-beam conditions

Because STEM uses a focused – i.e. converged – e^- beam, scattering in the sample gives a convergent beam electron diffraction pattern

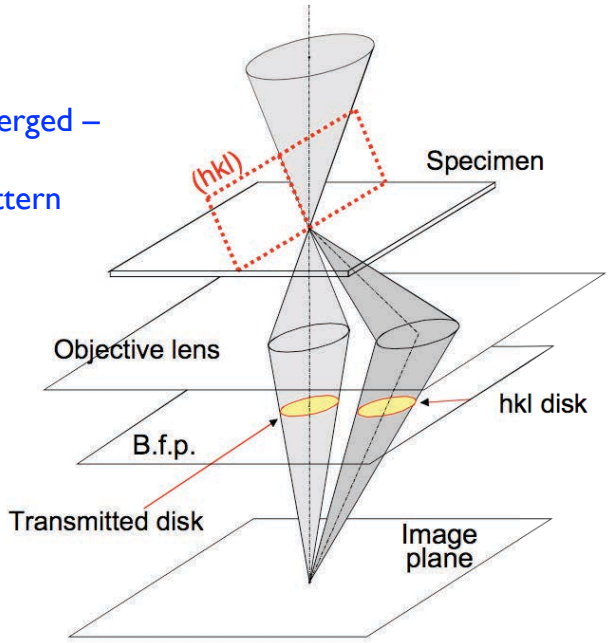

Figures by Jean-Paul Morniroli

Dedicated STEM design

- VG STEMs (1970s–1990s) and Nion UltraSTEMs (now) made "upside down" with the electron gun at the bottom
- Original STEMs had no lenses after samples; just detectors measuring integrated signal at different scattering angles, and energy-loss in transmitted electrons (EELS). Conceptually this still applies today.
- The properties of the probe-forming lens determine the image and its resolution – i.e. it is the image-forming lens. Therefore in the STEM community it is referred to as the "objective lens" and its aperture as the "objective aperture". Be careful with terminology, especially since on a combined TEM/STEM it is still the "condenser lens"!
- Often refer to fixed beam TEM as *CTEM* (conventional TEM)
- After sample detect only scattering angles – like far-field diffraction with no subsequent TEM image plane

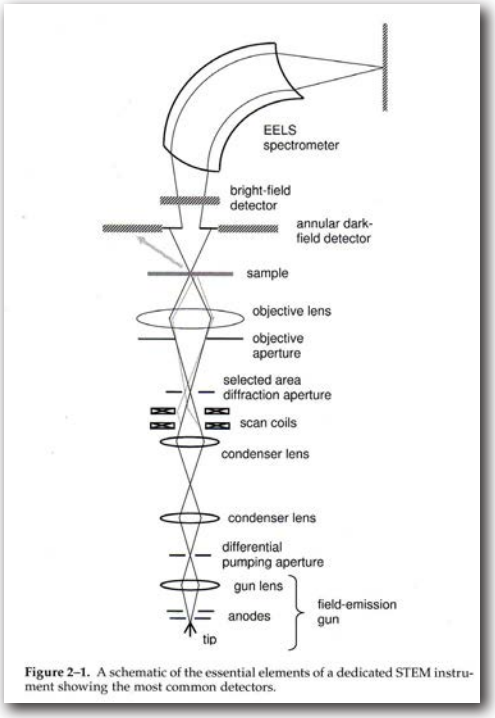

Figure 2–1. A schematic of the essential elements of a dedicated STEM instrument showing the most common detectors.

Dedicated STEM design

Early VG STEM

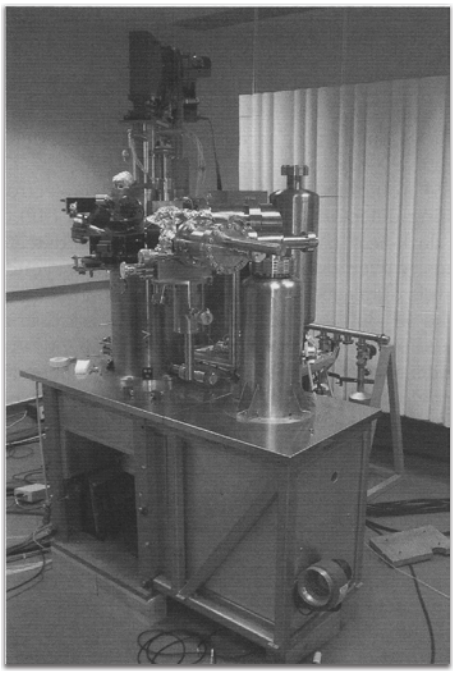

Nion UltraSTEM 200
(www.nion.com)

Dedicated STEM design

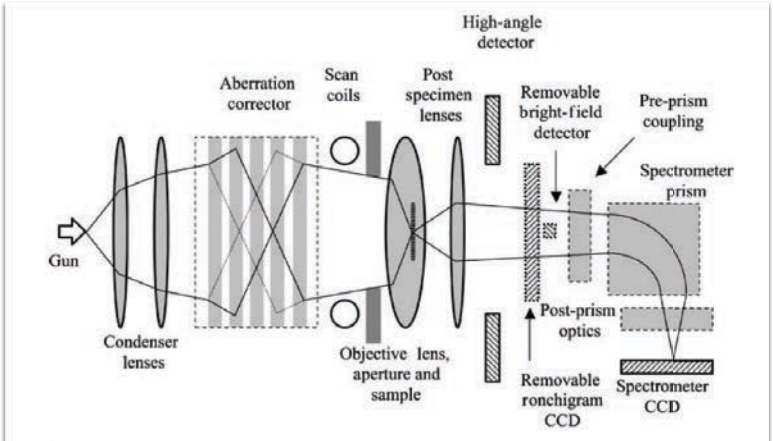

Figure 1 Simplified schematic of an aberration-corrected STEM; examples of electron trajectories are indicated. In the (quadrupole-octupole) aberration corrector, the different trajectories in the XZ and YZ planes are indicated with dotted and solid lines, respectively. The electrons are accelerated from the gun; condenser lenses are used to adjust the beam current and beam coherence and to couple to the aberration corrector. The objective lens focuses the probe, which is scanned across the sample by the scan coils. The high-angle detector collects electrons scattered to high angles. Removable bright field and Ronchigram detectors are shown as well as the important components of the spectrometer.

Varela *et al. Annu. Rev. Mater. Res.* 2005 **35** 539–69

TEM/STEM design

- Many modern field emission gun TEMs can also be used as STEMS (e.g. JEOL 2200FS, FEI Tecnai Osiris in CIME)
- STEM detectors are inserted in the back focal plane of the objective lens
- Use nano-beam (highly convergent) illumination – mini-condenser lens off
- Scan beam with TEM beam shift coils
- Modern TEMs STEM detectors send signal to computer acquisition software

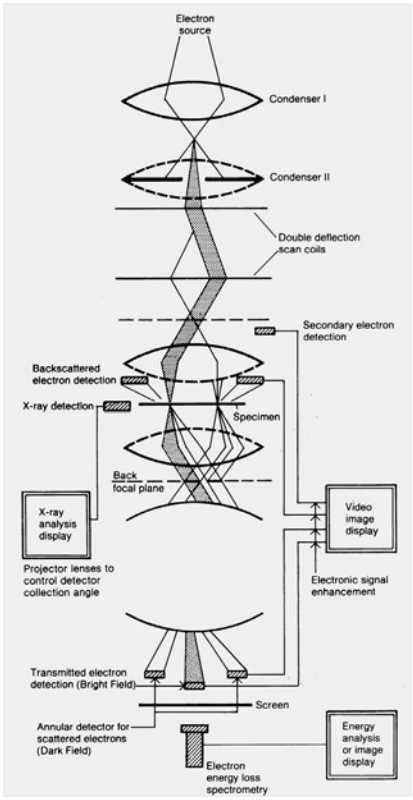

TEM/STEM design

Ray diagrams: TEM mode STEM mode

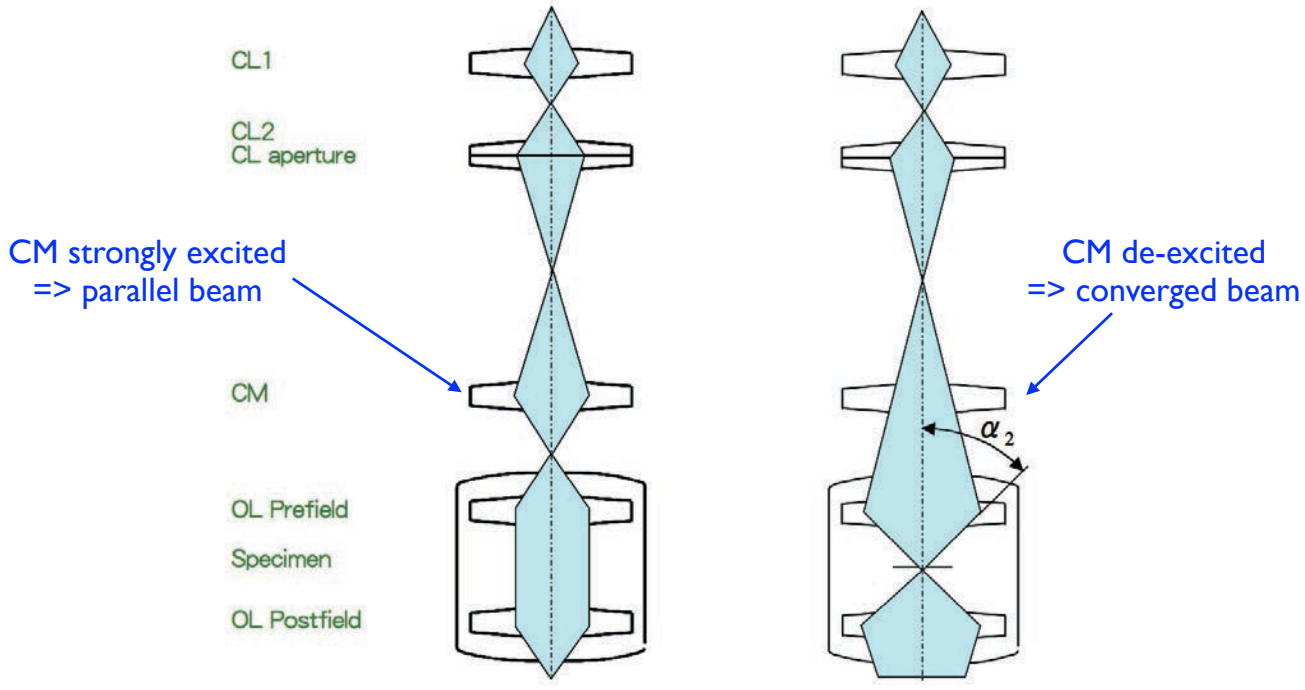

STEM imaging detectors

Focused e- probe scanned on sample; disc and annular detectors in back focal (diffraction) plane

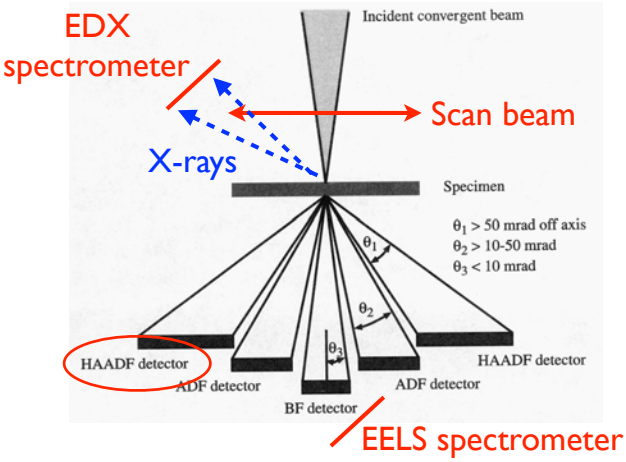

High-angle annular dark-field => compositional contrast:
intensity $\propto t Z^2$
(thickness t, atomic number Z)

Semi-conductor detector:

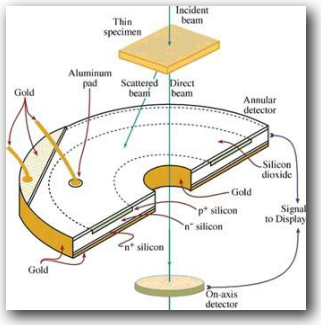

Scintillator photomultiplier (PMT) detector:

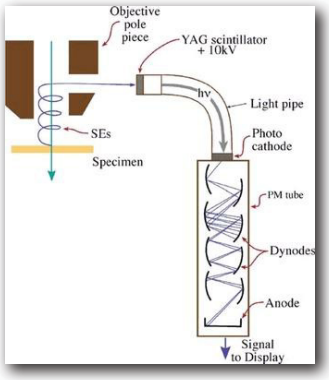

STEM detectors and signals

- With STEM we have the possibility to sample many different signals on different detectors, and can acquire that data with high spatial precision (atomic – nm scale)
- Therefore we can probe many different aspects of a sample; its structure, chemistry and physics
- For instance in CIME we have access to the following STEM detectors:
  - Bright-field; Annular bright-field; Annular dark-field; High angle annular dark-field (z-contrast); Secondary electron; Backscattered electron; Energy-dispersive X-ray (EDX) spectrometer; Electron energy-loss spectrometer (EELS); CCD camera; cathodoluminescence spectrometer
- Often we can acquire multiple signals in parallel, e.g.
  JEOL 2200FS: HAADF, EELS, CL
  Osiris: HAADF, DF4, DF2, BF/image + EDX spectrum
- This adds significantly to the capabilities of STEM

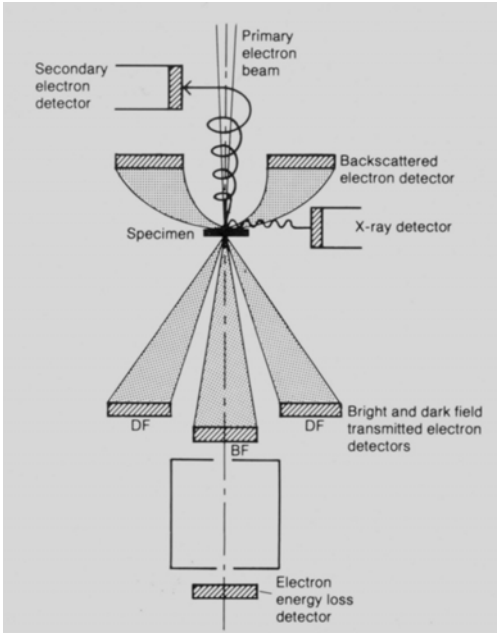

Reciprocity Theorem for equivalence of TEM and STEM bright-field imaging

Recprocity Theorem (from geometric optics): The amplitude of a wave a B due to an electron source at A is equal to the amplitude at A' due to a source at B'.

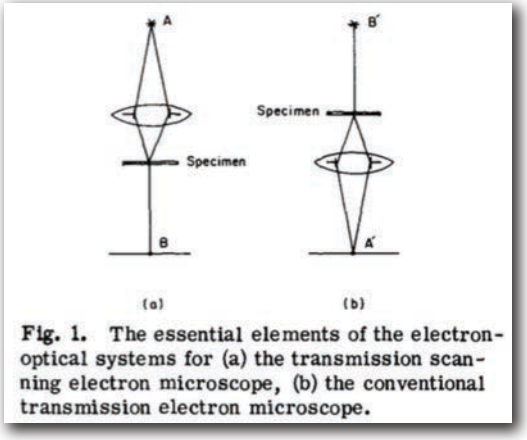

Fig. 1. The essential elements of the electron-optical systems for (a) the transmission scanning electron microscope, (b) the conventional transmission electron microscope.

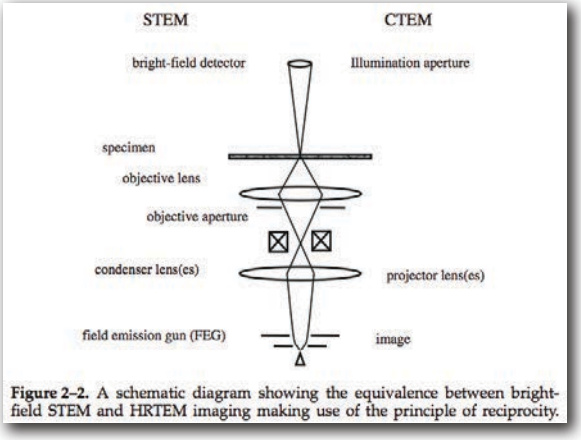

Figure 2–2. A schematic diagram showing the equivalence between bright-field STEM and HRTEM imaging making use of the principle of reciprocity.

J.M. Cowley *Applied Physics Letters* **15** (1969) 58

Convergence and collection angles

- The focused probe is a convergent electron beam. The BF and DF detectors are radially symmetric. Therefore all of them are characterised by angles – angle of convergence for the beam; collection of scattering angles for the detectors
- The convergence semi-angle of the probe is called α
- A collection semi-angle for a detector is called β
- Knowledge of these angles is important for STEM imaging

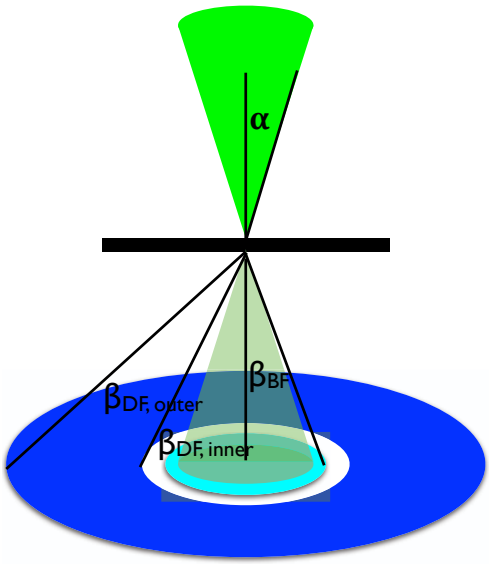

Quiz: for reciprocity with BF CTEM with a perfectly parallel incident beam, what collection angle do we need for the BF detector in STEM?

Bright-field & Annular dark-field detectors

- BF detector is a solid disc, dark-field detectors are ring shaped – i.e. annular – with certain inner and outer collection semi-angles β
- If the inner β is set-up to collect only diffracted beams we obtain a diffraction contrast dark-field image
- Diffraction intensity is an integration over all the selected beams – like an integration of multiple CTEM DF images

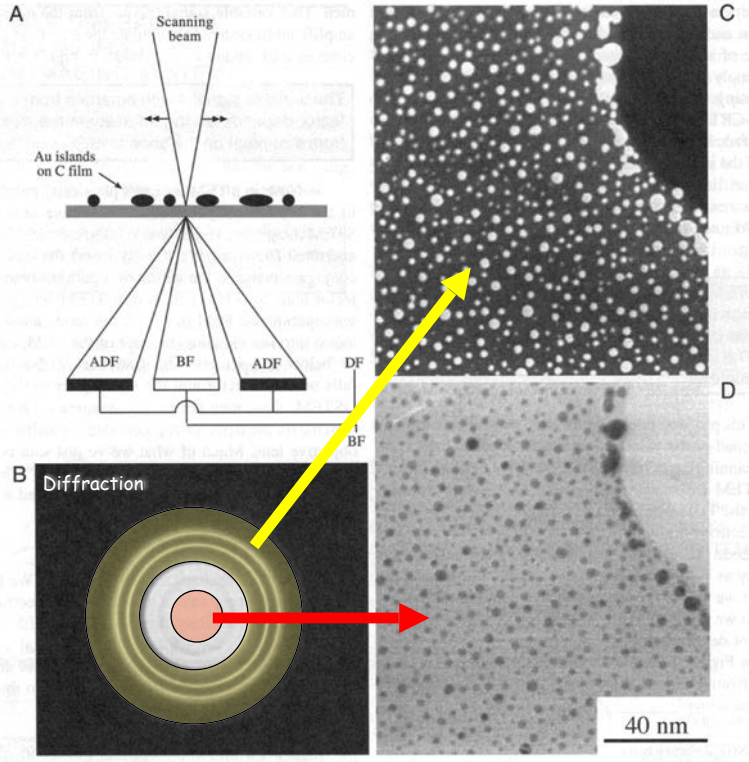

Diffraction contrast from BF & ADF signals

- As crystal tilts relative to incident beam/ changes thickness, the diffraction condition changes
- Defects also change diffraction condition
- Theses changes will change integrated signal on BF (red) and ADF (blue) detectors, and so change image intensity => diffraction contrast images

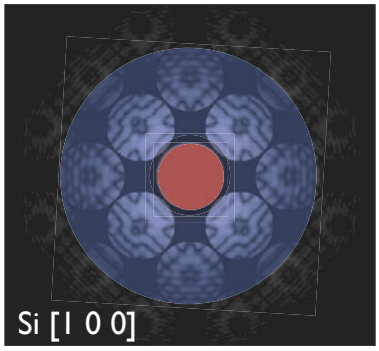

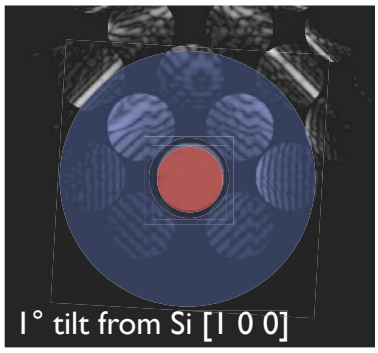

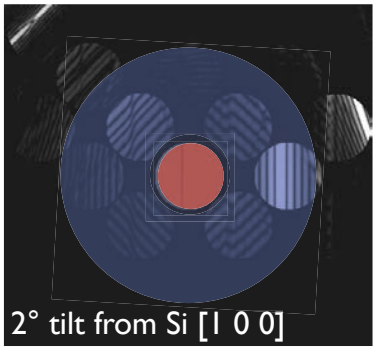

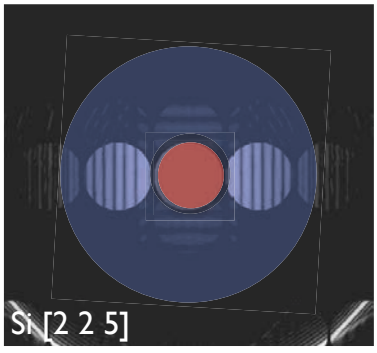

Bright-field STEM imaging example

- Polycrystalline ZnO thin-film on glass substrate
- Image rather equivalent to that from BF TEM, but bit more "averaging" of grain contrast

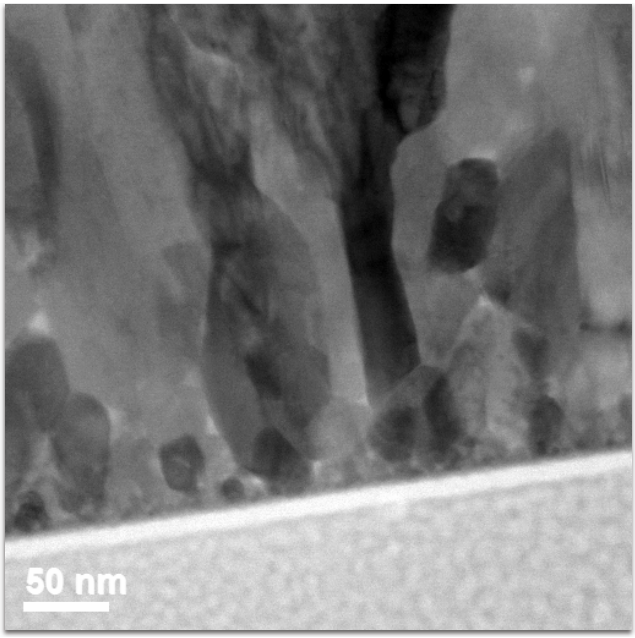

DF TEM vs ADF STEM imaging

- Photovoltaic stack (polycrystalline ZnO/proto-Si/polycrystalline-Si/ZnO)

DF TEM image: strong contrast, few grains have intensity

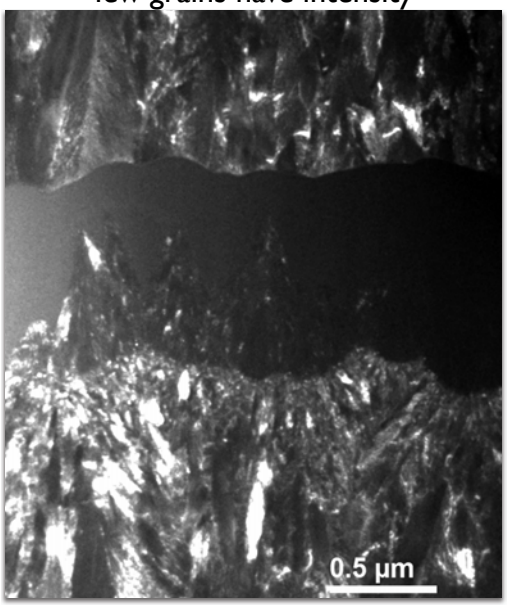

ADF STEM image: more grains have intensity, so more grain visibility & less contrast

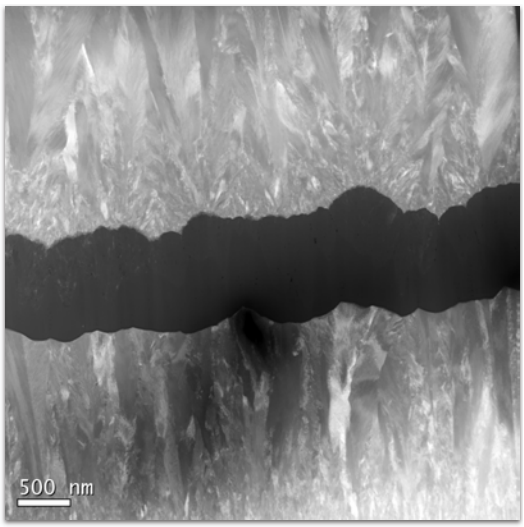

ADF STEM imaging example

- Photovoltaic stack (polycrystalline ZnO/proto-Si/polycrystalline-Si/ZnO)

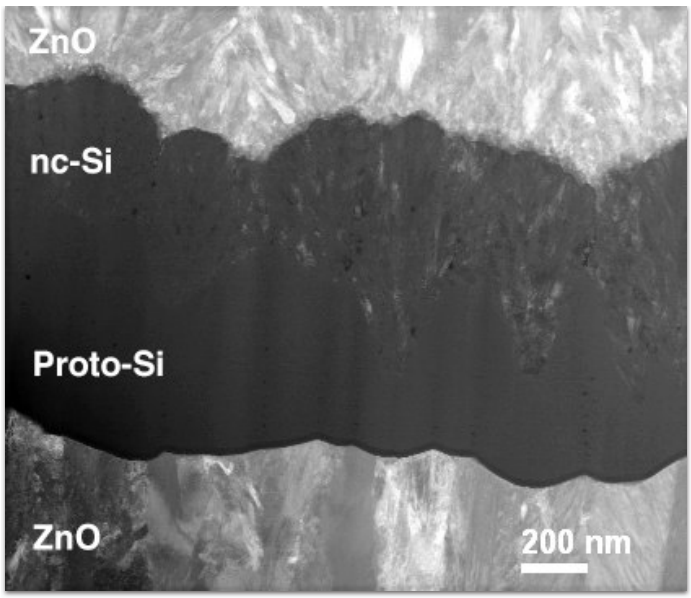

Visible: protocrystalline/crystalline Si interface, B-doped layer in proto-Si, voids

Influence of convergence angle

- Increasing convergence semi-angle α (e.g. by using larger condenser aperture) => diffraction discs overlap more
- Interference between discs can lead to phase contrast image

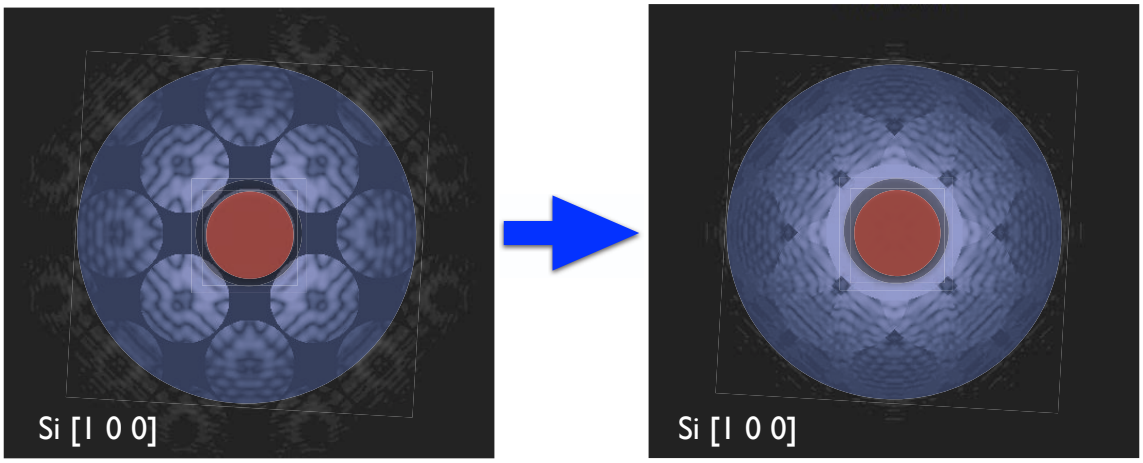

Influence of collection angle

- Increasing collection semi-angle β (e.g. by reducing camera length) => include diffracted beams on BF detector (integrated BF and DF intensity); ADF detector collects higher angle scattered beams

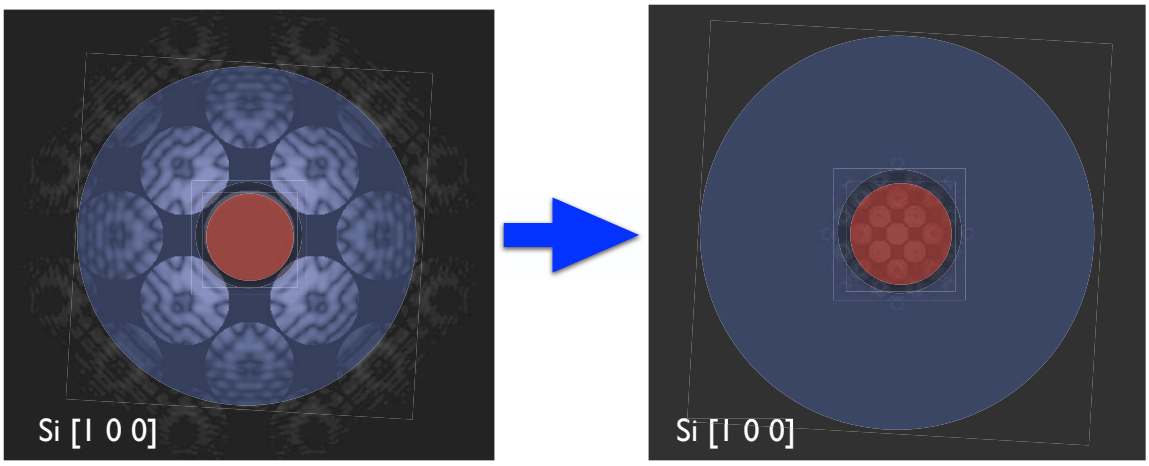

Bright-field/annular dark-field detectors
– Influence of camera length

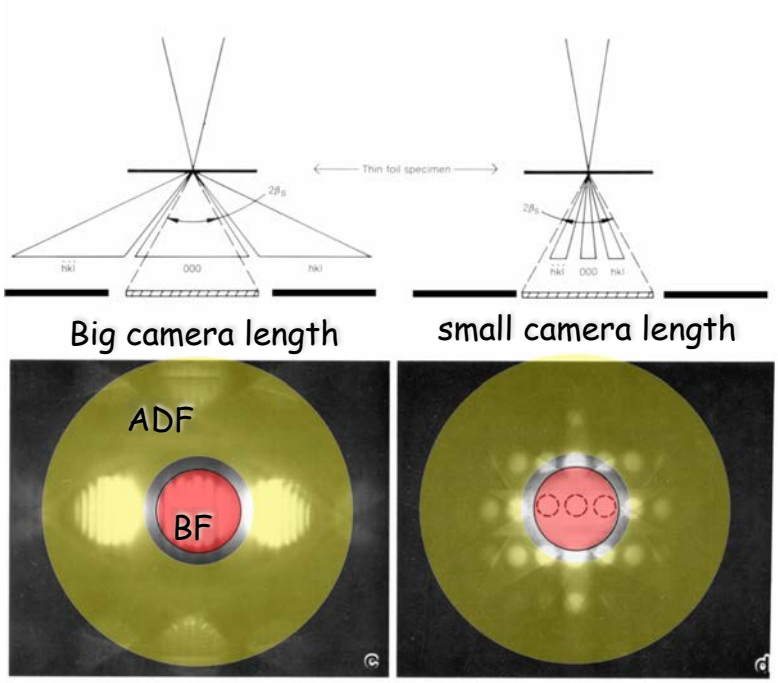

High-resolution BF STEM imaging

- Following from the theory of reciprocity, with a sufficiently small probe a BF detector can produce an image equivalent to a HR-TEM image.
- This is conditional on having CBED discs overlapping on the BF detector.
- No overlap is like BF CTEM imaging with only the direct beam chosen, so will give no fringes

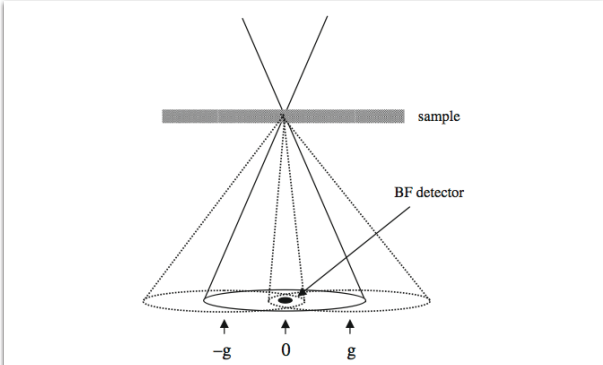

Figure 2–3. Diffraction of the coherent convergent beam by a specimen leads to diffracted discs. Where these discs overlap, interference will be seen. The bright-field detector is sensitive to interference between the direct beam and the two opposite diffracted beams.

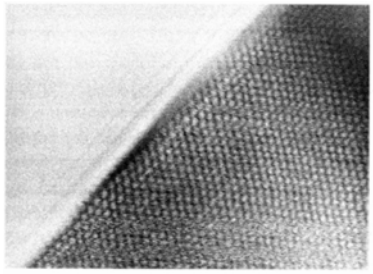

Figure 3. Bright-field STEM image of a small MgO crystal in [1 1 0] orientation [95].

Figure from Pennycook & Nellist
"Scanning Transmission Electron Microscopy"

Quiz: for a particular lattice spacing, how can we change convergence semi-angle α to have more disc overlap?

Fringes from annular dark-field

- The ADF detector can have overlapped fringes when the BF detector does not
- This will result in fringes in the ADF image even if there are none in the BF image
- Still assumes there is coherent elastic scattering; *what happens if we increase collection angle β?*

Figure 1–10. Schematic showing overlapping convergent beam discs for a case where the aperture radius is less than the diffraction angle λ/a. No overlaps occur for an axial detector, so no bright field lattice fringes are formed, but overlaps do lie on the annular detector, which makes possible atomic resolution ADF images.

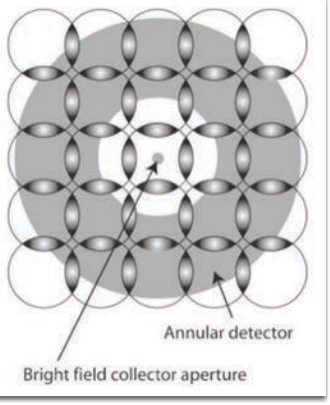

Figure from Pennycook & Nellist
"Scanning Transmission Electron Microscopy"

High angle annular dark-field (HAADF) imaging

Rutherford scattering

- Coulombic interaction with the electron cloud → low angle scattering
- Coulombic interaction with the nucleus → higher-angle scattering
- Rutherford cross-section for high-angle scattering by nucleus alone:

$$\sigma_R(\theta) = \frac{e^4 Z^2}{16(4\pi\varepsilon_0 E_0)^2} \frac{d\Omega}{\sin^4 \frac{\theta}{2}}$$

- Including screening and relativistic correction:

$$\sigma_R(\theta) = \frac{Z^2 \lambda_R^4}{64\pi^4 a_0^2} \frac{d\Omega}{\left[\sin^2\left(\frac{\theta}{2}\right) + \frac{\theta_0^2}{4}\right]^2}$$

- When scattering angle > screening parameter θ_0 the electron nucleus interaction is dominant (E_0 is in keV); e.g. Cu, 200 keV beam $\theta_0 \approx 25$ mrad

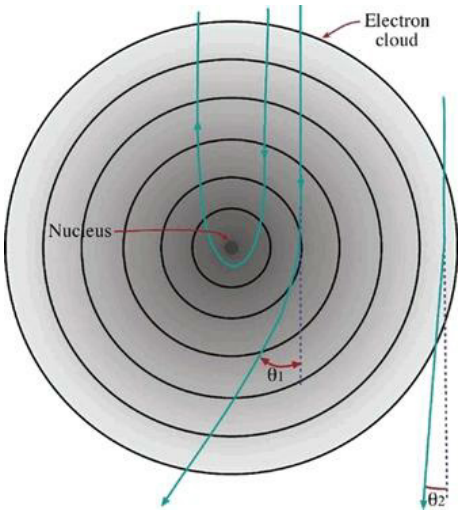

$$\theta_0 = \frac{0.117 Z^{1/3}}{E_0^{1/2}}$$

Rutherford → Mott scattering

- Rutherford: amplitude scattered by the wave vector, **s**, or electron scattering factor is:

$$f_{el}(s) = \frac{2}{a_0}\frac{Z^2}{s^2}$$

where Z is the atomic number and a_0 the Bohr radius
Scattering cross section is square of electron scattering factor

- Introduce screened coulomb potential to remove singularity as ***s*** tends to zero:

$$V(r) = \frac{Ze^2}{4\pi\varepsilon_0 r}\exp(-\mu r) \quad \text{to give:} \quad f_{el}(s) = \frac{2Z}{a_0(s^2+\mu^2)}$$

- While screening parameter, μ, attempts to incorporate extra scattering due to atomic electrons, this can be done exactly with Mott formula:

$$f_{el}(s) = \frac{2}{a_0}\frac{[Z - f_X(s)]}{s^2}$$

where fx(s), the X-ray scattering factor, is the Fourier transform of e⁻ charge density and describes coulomb scattering by atomic electrons

Amali & Rez Microsc. Microanal 3 (1997) 28–46

High-angle annular dark field (HAADF)

- By using a detector/ camera length combination that gives large collection angles (e.g. β >80–100 mead) we can more or less collect the Mott (Rutherford) -scattered exclusively
- These angles are typically too large for coherent elastic scattering (i.e. diffraction)
- This is called high-angle annular dark-field (HAADF)

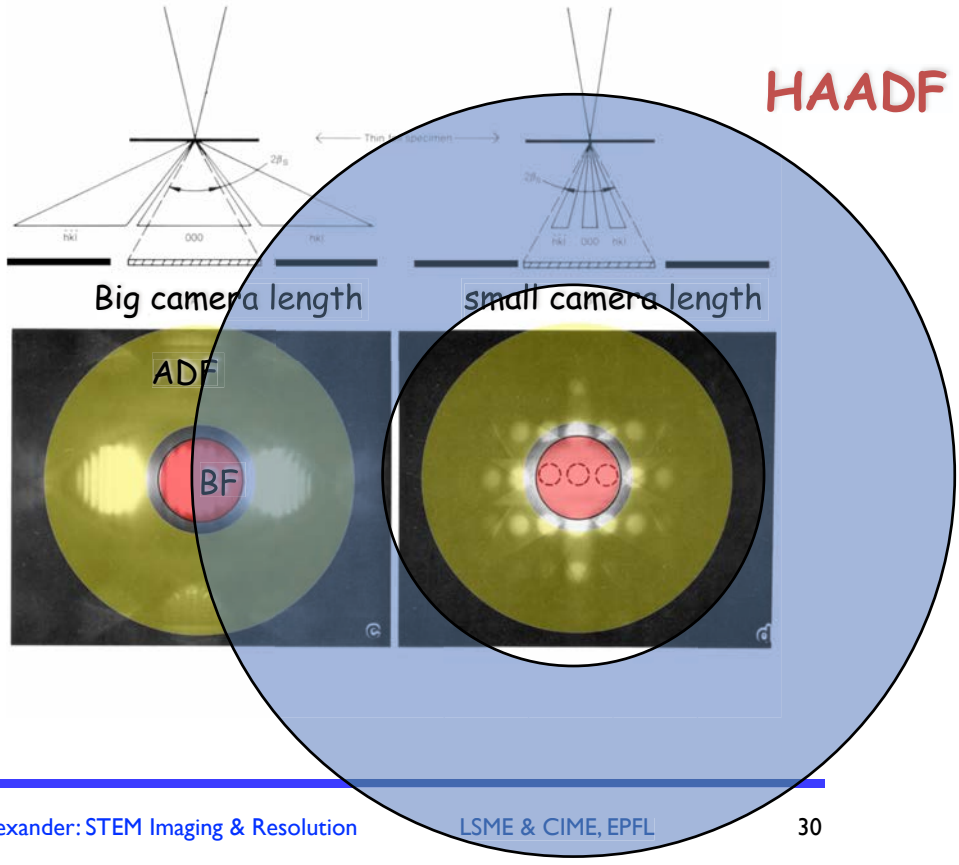

HAADF/Z-contrast imaging

- By collecting only Mott (Rutherford)-scattered electrons, the HAADF detector produces an image which (ideally) gives an intensity:
  $I \propto tZ^2$
  for thickness t, average atomic number Z
- Diffraction contrast is eliminated (or at least much reduced…)
- In reality:
  $I \propto tZ^{1.6–2}$

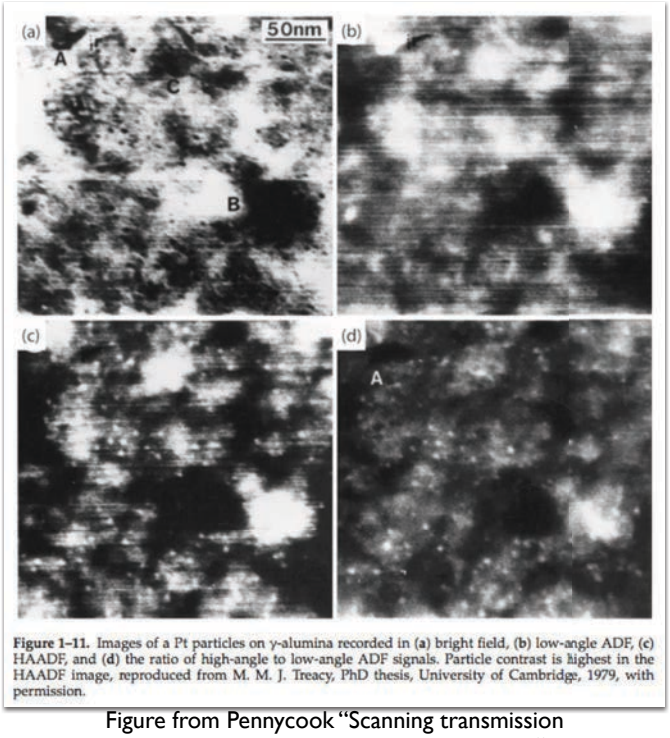

Figure 1–11. Images of a Pt particles on γ-alumina recorded in (a) bright field, (b) low-angle ADF, (c) HAADF, and (d) the ratio of high-angle to low-angle ADF signals. Particle contrast is highest in the HAADF image, reproduced from M. M. J. Treacy, PhD thesis, University of Cambridge, 1979, with permission.

Figure from Pennycook "Scanning transmission electron microscopy : imaging and analysis"

HAADF/Z-contrast imaging

Z-contrast examples:

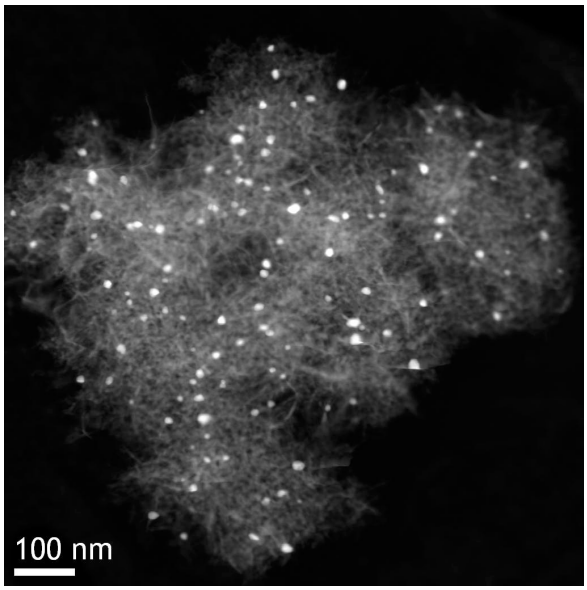

Pt catalyst on Al_2O_3

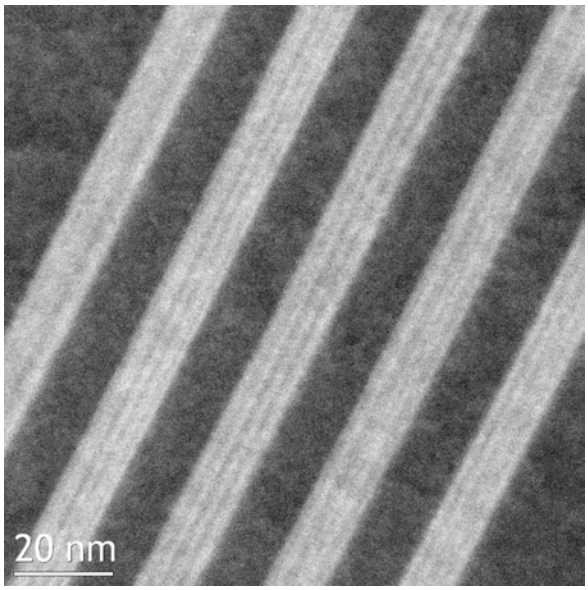

Si-Ge/Si multilayer

HAADF/Z-contrast imaging

Z-contrast examples:

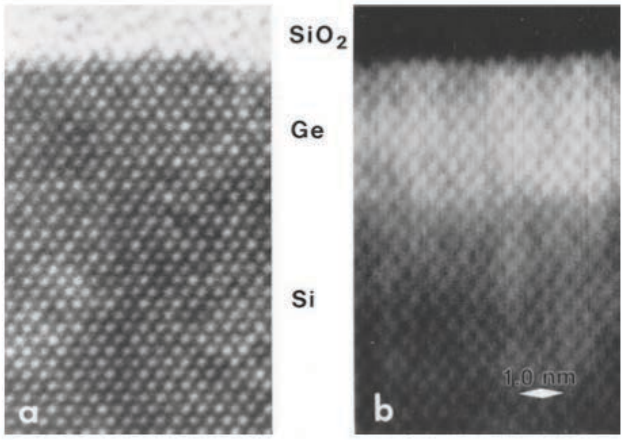

Figure 1–16. Images of a Ge film grown epitaxially on Si by an implantation and oxidation method. (**a**) Conventional TEM image from a JEOL 200CX, (**b**) Z-contrast image obtained with a VG Microscopes HB501UX clearly delineating the Ge layer, reproduced from Pennycook (1989a).

Figure from Pennycook "Scanning transmission electron microscopy : imaging and analysis"

HAADF/Z-contrast imaging

Z-contrast examples:

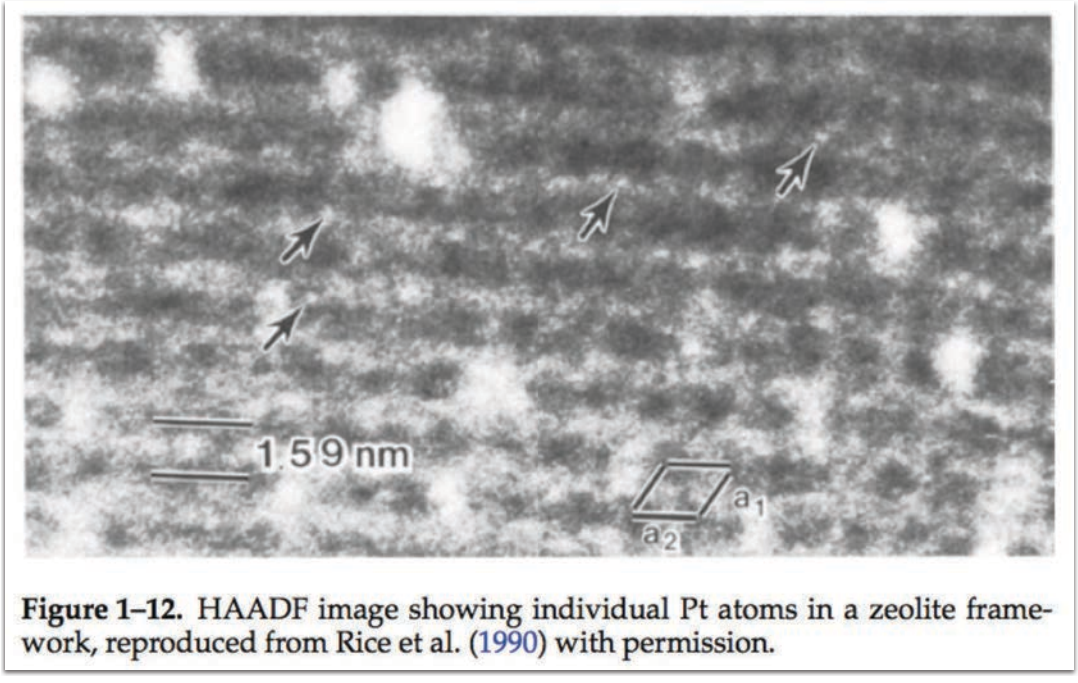

Figure 1–12. HAADF image showing individual Pt atoms in a zeolite framework, reproduced from Rice et al. (1990) with permission.

Figure from Pennycook "Scanning transmission electron microscopy : imaging and analysis"

Coherent vs Incoherent imaging

- In the 1970s, biologists Engel et al. and Misell et al. proved that the integration of signals on an ADF detector represents a convolution of intensities instead of amplitudes:

$$I(\mathbf{R}_0) = \int |\varphi(\mathbf{R})|^2 \, |P(\mathbf{R} - \mathbf{R}_0)|^2 \, d\mathbf{R}$$

- The fundamental equation for incoherent images is therefore obtained:

$$I(\mathbf{R}_0) = |\varphi(\mathbf{R}_0)|^2 \otimes |P(\mathbf{R}_0)|^2$$

- Compared to coherent – i.e. phase contrast – imaging, incoherent imaging has some specific (useful!) characteristics:
  - No image contrast inversion with defocus
  - "Camera-like characteristics"
  - Broad optical transfer function

Optical transfer function of incoherent imaging

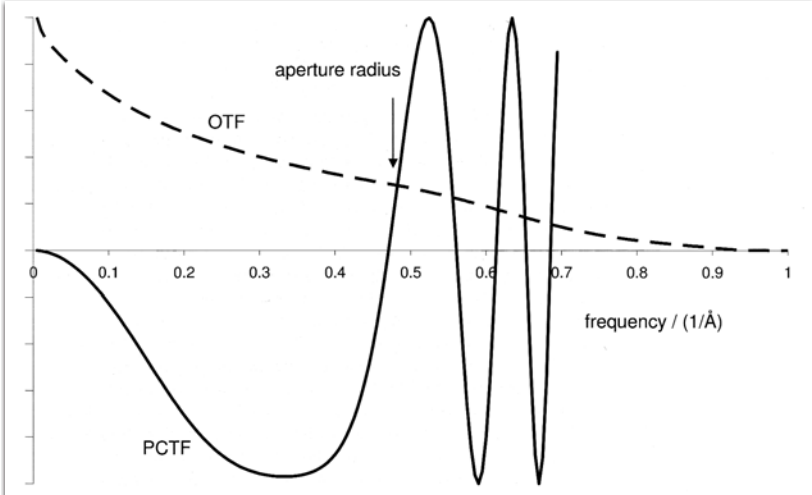

Figure 2–12. A comparison of the incoherent object transfer function (OTF) and the coherent phase-contrast transfer function (PCTF) for identical imaging conditions (V = 300 kV, C_S = 1 mm, z = −40 nm).

- Incoherent imaging gives a better spatial resolution than coherent imaging
- This was proved by Lord Rayleigh in 1896 (Phil. Mag. **42**, p. 167); the Rayleigh criterion for resolution basically applies

"Scanning Transmission Electron Microscopy", P.D. Nellist, in *Science of Microscopy Vol. 1*, Springer 2007

Spatial resolution of incoherent imaging

- The above results mean that an ADF STEM image has a fundamentally improved spatial resolution compared to its BF counterpart
- Only realised on materials science samples once HAADF detector introduced since the lower-angle ADF detector collects too much coherent diffraction signal to achieve incoherency
- In contrast Rutherford-scattered electrons are fundamentally incoherent; this scattering destroys the phase relationship

Figure from Pennycook "Scanning transmission electron microscopy : imaging and analysis"

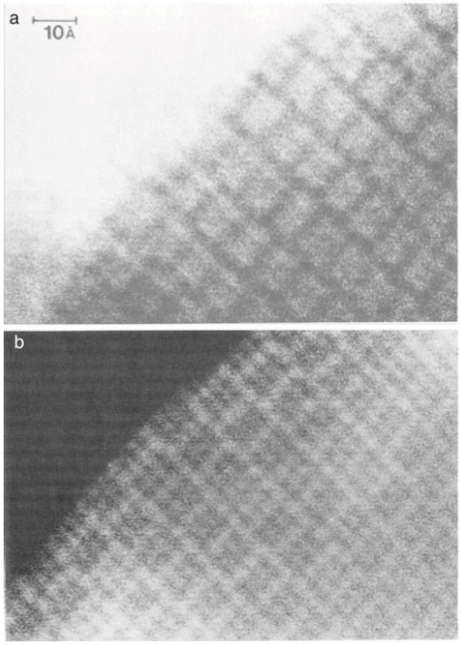

Figure 1–14. (**a**) Bright field and (**b**) ADF images of $Ti_2Nb_{10}O_{29}$ showing improved atomic resolution detail in the dark field image, reproduced from Cowley (1986b) with permission.

The electron source and probe

- To benefit from these advantages of STEM we need a very well focused electron probe
- This requires: good optics and a small source
- *Why do we need a small source?*
- A field emission gun is mandatory: Albert Crewe (and VG) used cold field emission guns
- Cold field emission gun has smaller source, higher brightness than warm, Schottky field emission gun; becoming popular again (Nion, JEOL ARM, Hitachi)

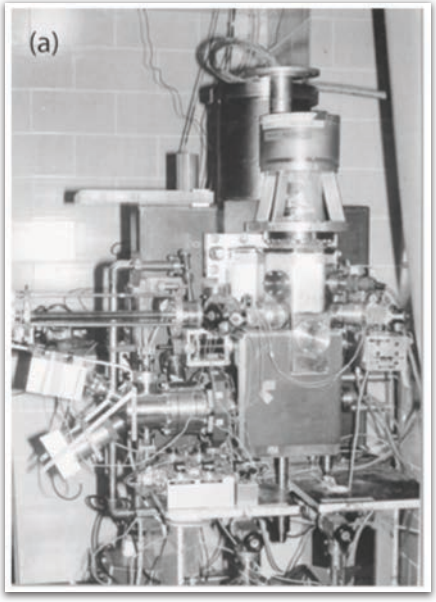

The electron source and probe

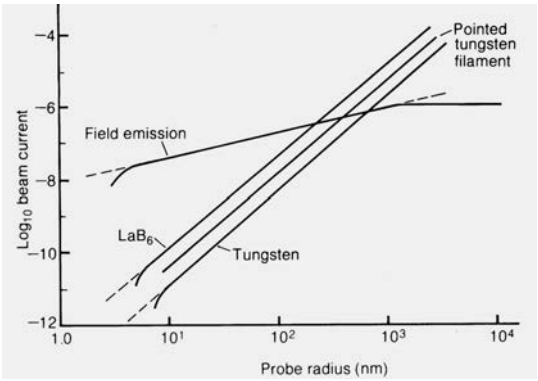

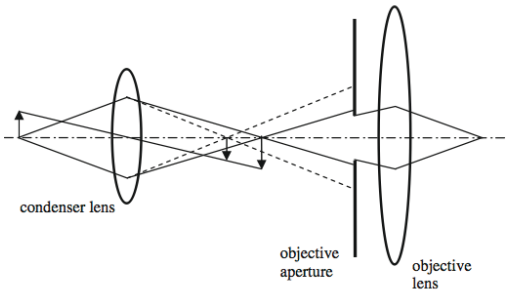

Figure 2–6. Increasing the strength of the condenser lens to provide greater source demagnification leads to greater loss of current at the objective aperture and less probe current.

The electron Ronchigram

The Electron Ronchigram as we see it

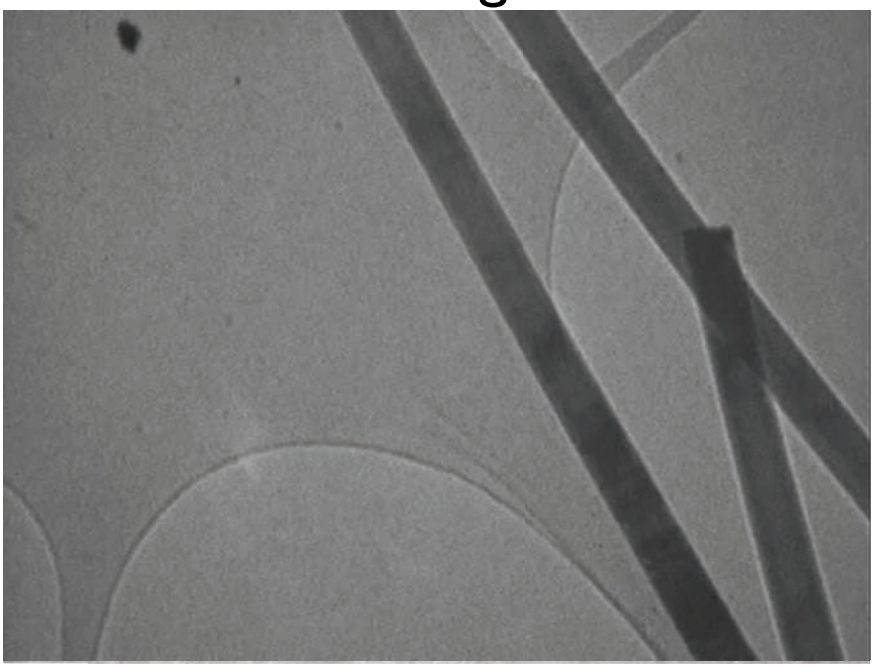

- STEM mode; fix the probe; large/no aperture in probe-forming lens
- Record 2-D image of intensity in diffraction (i.e. STEM detector) plane
- See "shadow image" of sample in the diffraction disc

Basics of shadow image formation

Assuming perfect optics

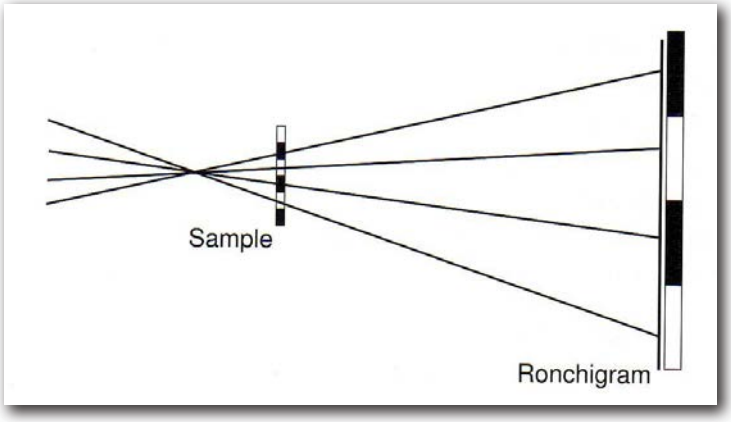

At overfocus the STEM detector plane is a shadow image of the sample
Magnification $M = d_{\text{probe-detector}}/d_{\text{probe-sample}}$

At underfocus the image will be magnified, but also *inverted*

Ronchigram is similar to defocused TEM diffraction pattern, blending image information with scattering angles

Diagram from: "Scanning Transmission Electron Microscopy", P.D. Nellist, in *Science of Microscopy Vol. 1*, Springer 2007

Shadow image formation in the presence of large spherical aberration

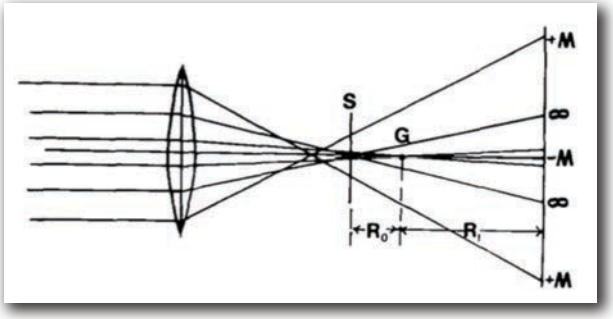

J.M. Cowley *Ultramicroscopy* **4** (1979) 413

Gaussian focus *G*;
paraxial magnification $M = R_i/R_0$

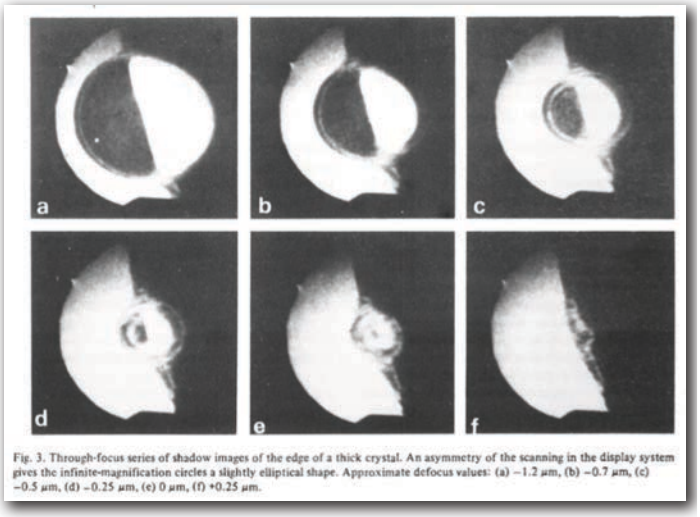

Fig. 3. Through-focus series of shadow images of the edge of a thick crystal. An asymmetry of the scanning in the display system gives the infinite-magnification circles a slightly elliptical shape. Approximate defocus values: (a) −1.2 μm, (b) −0.7 μm, (c) −0.5 μm, (d) −0.25 μm, (e) 0 μm, (f) +0.25 μm.

J.M. Cowley *Ultramicroscopy* **4** (1979) 435

Underfocus: infinite magnification for rays that cross at S

Gaussian and overfocus: magnification decreases smoothly for larger angles

Radii and azimuths of infinite magnification

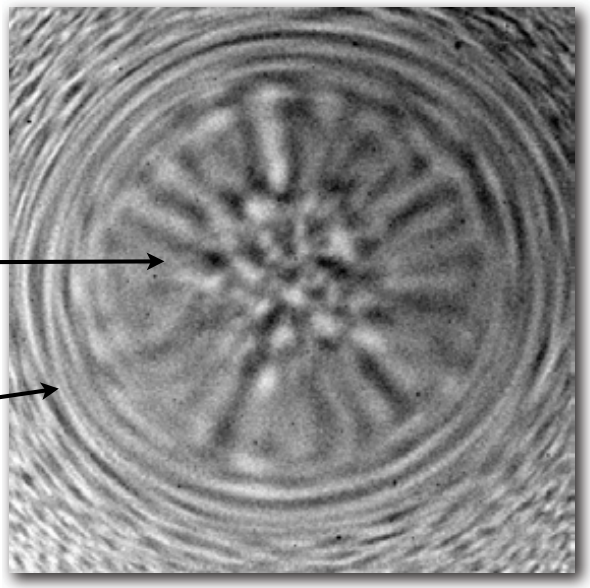

- The underfocus Ronchigram shows infinite magnification at more than one scattering angle
- In fact there are radii (radial spokes) and tangential azimuths (rings) of infinite magnification
- Why is this?

Radii and azimuths of infinite magnification

Phase shift due to aberration in *Front Focal Plane* of "objective" lens (TEM = "condenser"):

$$\chi(\boldsymbol{K}) = \left(\pi z\lambda|\boldsymbol{K}|^2 + \frac{1}{2}\pi C_s\lambda^3|\boldsymbol{K}|^4\right) \quad \text{for defocus } z\text{, wavevector } \boldsymbol{K}\text{, where } \boldsymbol{K} = \frac{\theta}{\lambda}$$

From this, Cowley derived that:

In 1-D: $$M' = \frac{M}{1 + C_s\lambda^2|\boldsymbol{K}|^2/z}$$

M: magnification for $C_s = 0$; M': actual magnification

– *consistent with overfocus image, however infinite magnification would only occur at:* $$|\boldsymbol{K}|^2 = \frac{-z}{C_s\lambda^2}$$

However in 2-D derivation there are *two* critical angles:

Radial magnification is infinite for: $$|\boldsymbol{K}|^2 = \frac{-z}{3C_s\lambda^2}$$

Circumferential magnification is infinite for: $$|\boldsymbol{K}|^2 = \frac{-z}{C_s\lambda^2}$$

J.M. Cowley *Journal of Electron Microscopy Technique* **3** (1986) 25

So why is it called the "Ronchigram"?

While not referred to as the Electron Ronchigram in Cowley's first papers describing the phenomena, by 1986 this term was used by analogy to the optical tests for aberrations developed by Vasco Ronchi [1-3]

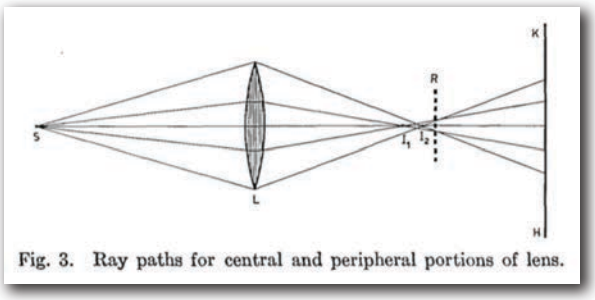

Fig. 3. Ray paths for central and peripheral portions of lens.

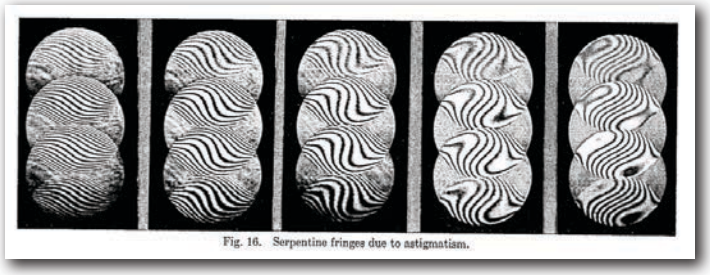
Fig. 16. Serpentine fringes due to astigmatism.

V. Ronchi *Applied Optics* **3** (1964) 437

If we are rigorous Electron Ronchigram only refers to scattering from periodic objects; however the term is used more generally for the figure from amorphous phase too

[1] *Ultramicroscopy* **4** (1979) 413; [2] *Ultramicroscopy* **4** (1979) 435; [3] *Journal of Electron Microscopy Technique* **3** (1986) 25

Aligning STEM mode with the Ronchigram

Correcting astigmatism: characteristic "American football" when astigmatic

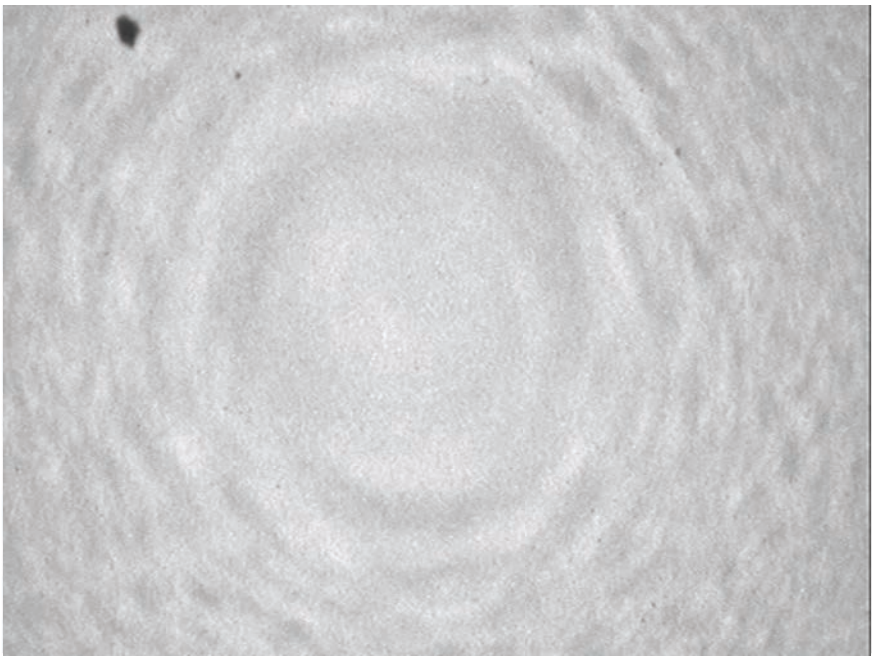

Focusing with the Ronchigram

From criterion that phase shift $\chi(\boldsymbol{K})$ must not depart more than π/4 from 0, it is found that for a given C_s of "objective" lens optimal defocus is:

$$z = -0.71\lambda^{1/2}C_s^{1/2}$$

Allowing "objective" aperture with radius of:

$$\alpha = 1.3\lambda^{1/4}C_s^{-1/4}$$

At optimum defocus and with correct aperture size, the probe FWHM is given by:

$$d = 0.4\lambda^{3/4}C_s^{1/4}$$

"Scanning Transmission Electron Microscopy", P.D. Nellist, in *Science of Microscopy Vol. 1*, Springer 2007

Focusing with the Ronchigram

- In practice:
  - Reduce under-focus until infinite-magnification rings are of minimum diameter => optimum defocus (c.f. Scherzer defocus in HR-TEM)

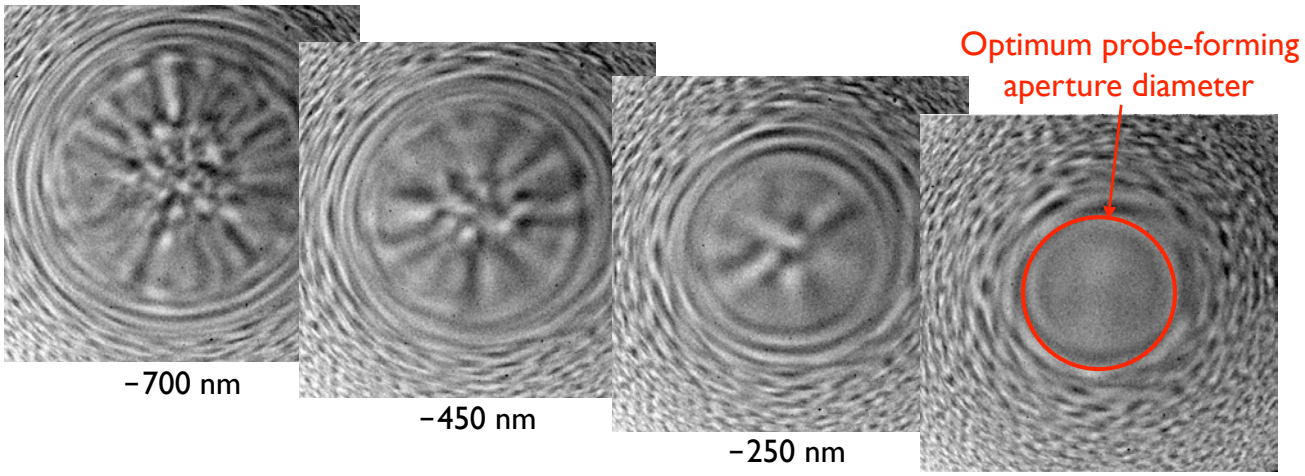

  - Fit probe-forming aperture to the "sweet spot" region of constant phase within this diameter

Increasing probe-forming aperture size

- What happens if we increase probe-forming aperture beyond the sweet-spot?
- Look at streak images of the electron probe from Osiris going from $\alpha \approx 11$ mrad (left) to $\alpha \approx 16$ mrad (right)
- The sweet-spot gives a peak in the middle which does not change much; in contrast the tails go up enormously from putting in these aberrations => more signal but not from where we want

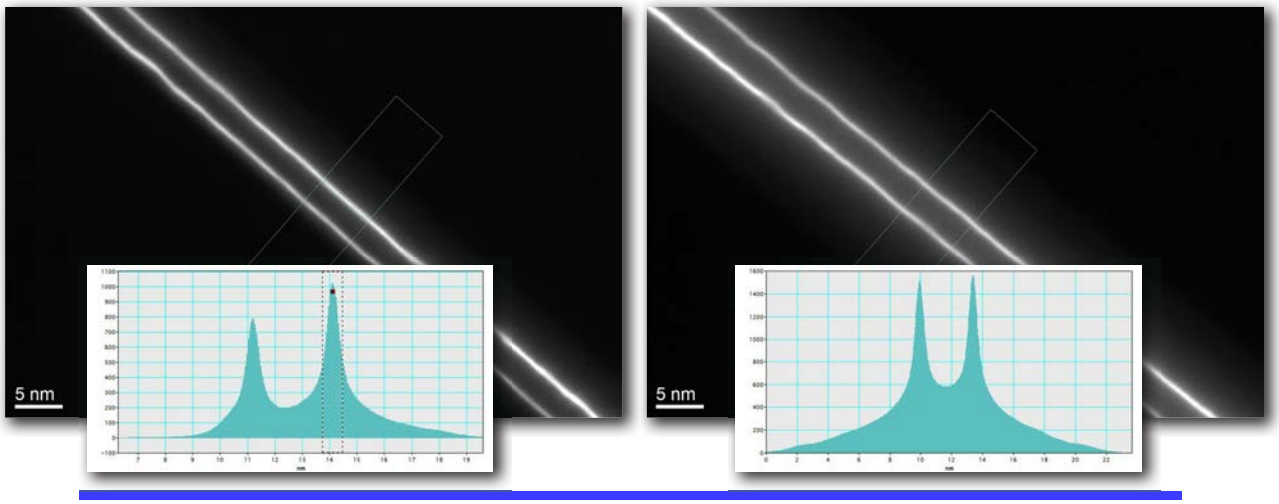

Cs-Aberration correction in STEM

- First STEM aberration corrector installed on VG by Nion (Krivanek); quadrupole-octopole design. This is now used on Nion UltraSTEM.

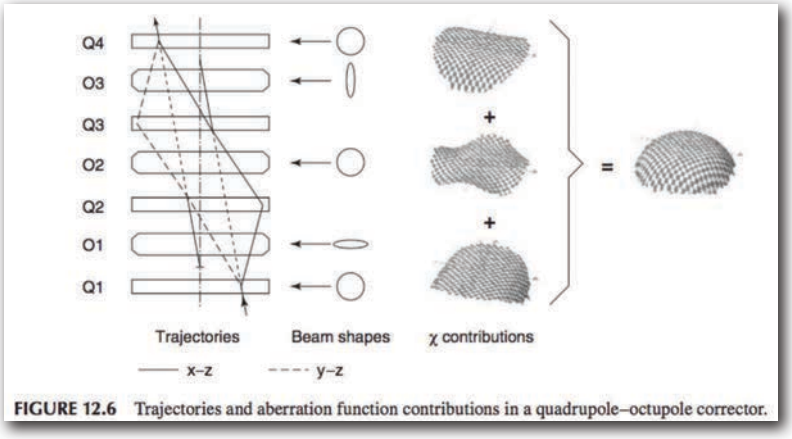

FIGURE 12.6 Trajectories and aberration function contributions in a quadrupole–octupole corrector.

- CEOS aberration corrector also used for aberration-corrected STEM on many instruments (FEI, JEOL, Hitachi)

Krivanek et al Aberration Correction in Electron Microscopy Handbook of Charged Particle Physics 2009 pp 601–641

Effect of aberration-correction on sweet spot

- At optimum defocus aberration correction produces a sweet spot (region of flat phase) with much greater diameter; *c.f. effect of Cs-correction on CTF in HR-TEM*
- E.g. for HT 100 kV, Cs 1.0 mm, sweet spot has:
  With no correction $\alpha_{max} = 1.5(\lambda/C_3)^{1/4}$ = 11.6 mrad
  With C_5/C_5 (as shown) correction α_{max} = 40 mrad

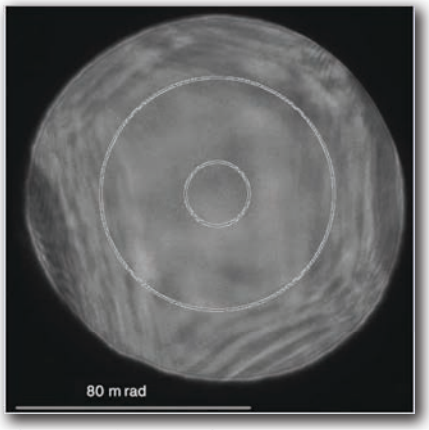

- Demagnification of virtual source size by the objective (probe-forming) lens increases in proportion with illumination angle (assuming this does not exceed sweet spot diameter) => Probe size decreases as α_{max}^{-1}
- Using larger probe-forming aperture also improves resolution slightly because diffraction limit reduced
- *Quiz: as probe-forming aperture increased, what happens to: a) beam current? b) focal depth?*

Cs-corrected Ronchigram movie

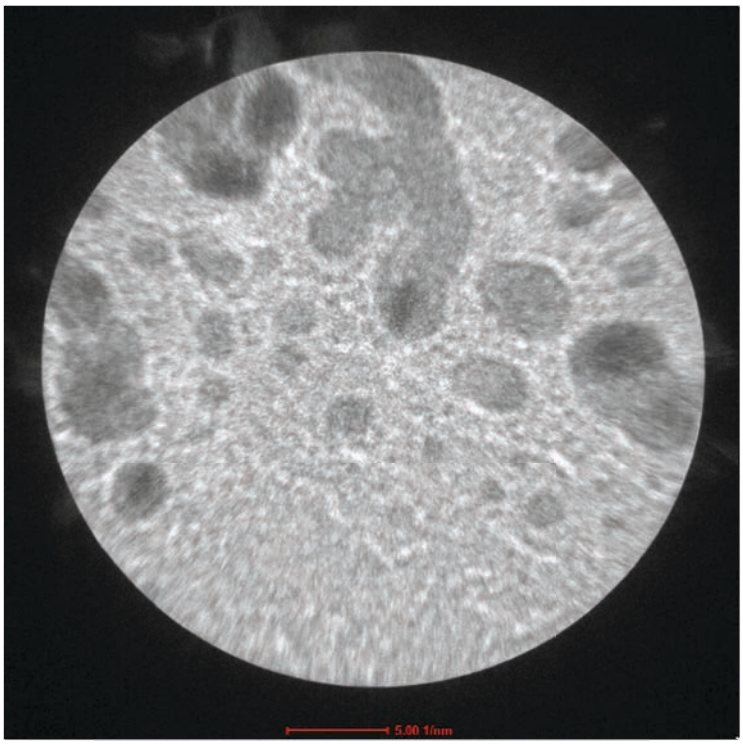

Recorded from FEI Titan Themis at CIME

Cs-corrected Ronchigram movie

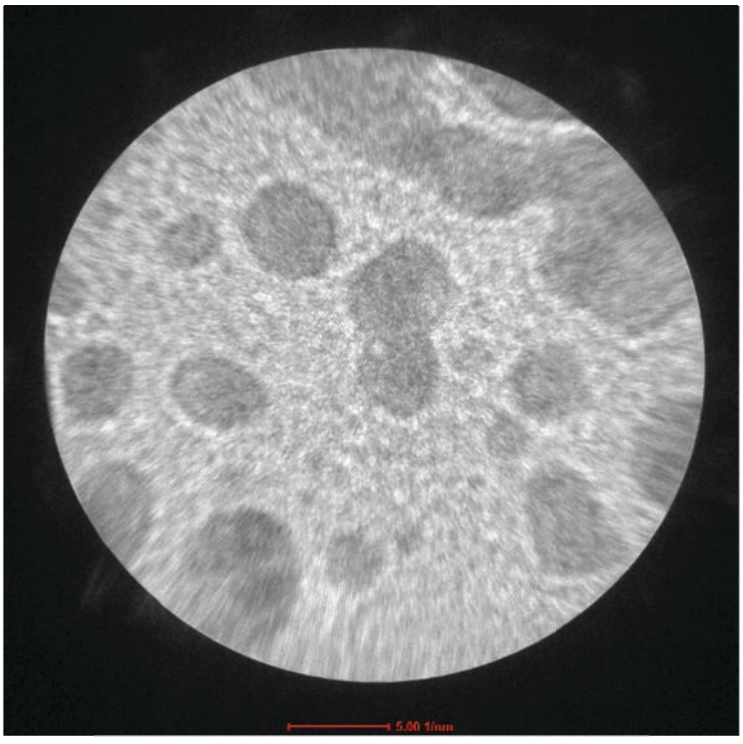

Recorded from FEI Titan Themis at CIME

Aberration-corrected examples

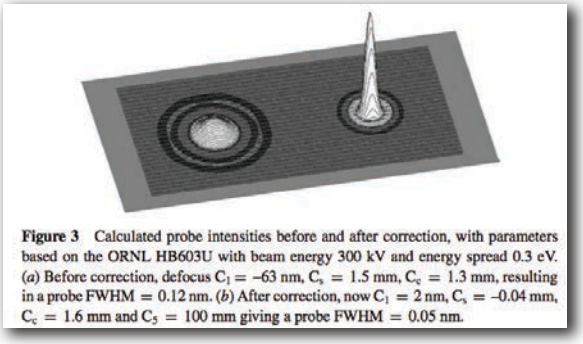

Figure 3 Calculated probe intensities before and after correction, with parameters based on the ORNL HB603U with beam energy 300 kV and energy spread 0.3 eV. (*a*) Before correction, defocus $C_1 = -63$ nm, $C_s = 1.5$ mm, $C_c = 1.3$ mm, resulting in a probe FWHM = 0.12 nm. (*b*) After correction, now $C_1 = 2$ nm, $C_s = -0.04$ mm, $C_c = 1.6$ mm and $C_5 = 100$ mm giving a probe FWHM = 0.05 nm.

Varela et al. Annu. Rev. Mater. Res. 2005 **35** 539–569

Z-contrast image: "direct" interpretation, but light O columns not visible.

BF detector gives simultaneous phase contrast image equivalent to HR-TEM image; O columns visible but similar problems to interpret as HR-TEM image

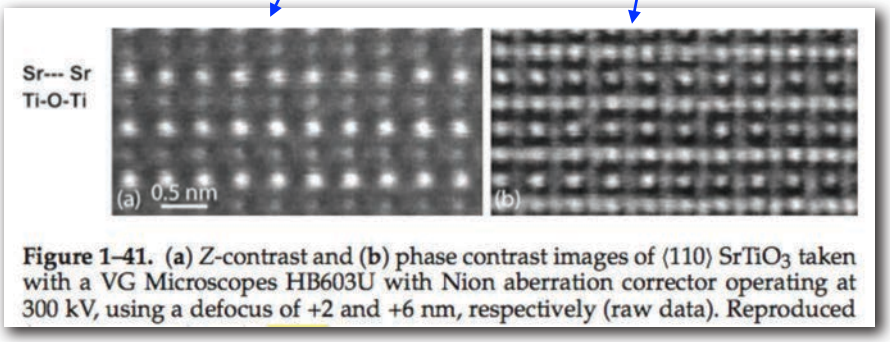

Figure 1–41. (a) Z-contrast and (b) phase contrast images of (110) $SrTiO_3$ taken with a VG Microscopes HB603U with Nion aberration corrector operating at 300 kV, using a defocus of +2 and +6 nm, respectively (raw data). Reproduced

Pennycook "Scanning Transmission Electron Microscopy" Chapter 1

Theory & simulation of HAADF imaging

- Mott (Rutherford) scattering applies to isolated atoms, or atoms in single atomic layer lattice (e.g. graphene) imaged with atomic resolution; also reasonable assumption for nanoscale clusters/particles imaged without atomic resolution
- Thin crystalline samples imaged with atomic resolution on zone axis: HAADF imaging considered to involve two scattering processes:
  - Propagation of electron wave across crystal lattice as Bloch waves (solution of Schrödinger's equation for electron wave in electrostatic potential of lattice)
  - Quasi-elastic scattering of 1s Bloch wave by lattice vibrations, i.e. phonons. This is termed:
    Thermal Diffuse Scattering (TDS)

Theory & simulation of HAADF imaging

- Bloch waves: in 2 beam condition electron wave propagates as 2 Bloch waves: type-1 with electron density peaked on atomic columns; type-2 with electron density peaked between atomic columns
- Two waves travel with different speeds (more negative potential on atomic column leads to type-1 propagating faster) ⟹ Phase difference
- On exit from crystal surface, waves recombine to give direct and diffracted beam
- Phase difference produces dynamical scattering effects
- Zone axis: *m* diffracted beams ⟹ *m* Bloch waves
- 1s Bloch wave has peaked electron density on atomic column (atomic nuclei); more strongly "absorbed" (lost due to de-phasing)

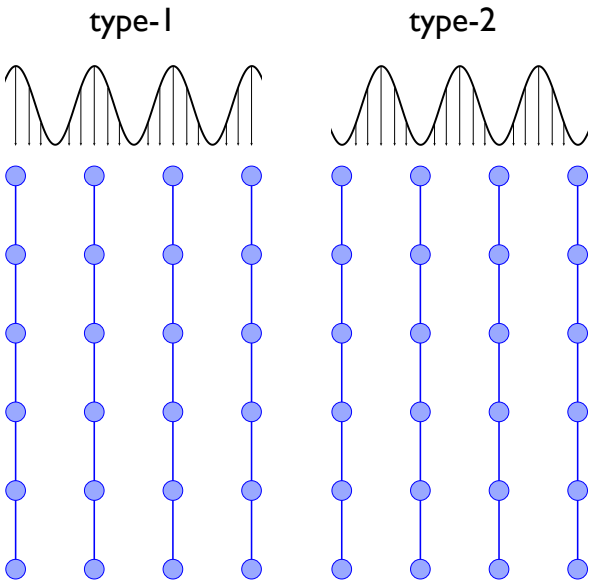

Theory & simulation of HAADF imaging

- Crystal potential perturbed by atomic vibrations (phonons)
- Scattering behaviour of incident electrons perturbed: this gives electron-phonon interactions
- Perturbation potential is not periodic; gives "incoherent" diffuse scattering between Bragg beams – the TDS
- Account for thermal vibrations with crystal potential V having static V_0 and time-dependent ΔV components:

$$V(\mathbf{r}, t) = V_0(\mathbf{r}) + \Delta V(\mathbf{r}, t).$$

- V_0 responsible for Bragg beams; ΔV for TDS
- When atom displaced ΔV is narrow, indicating that TDS is *localised to nuclear sites*

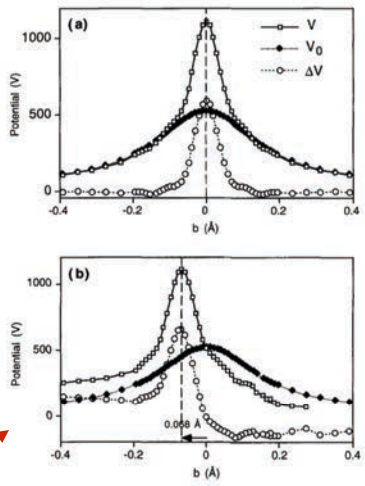

Z.L. Wang Phil. Mag. B 79 (1999) 37–48;
Z.L. Wang *Elastic and Inelastic Scattering in Electron Diffraction and Imaging*, Plenum Press, p. 150–160

Theory & simulation of HAADF imaging

- 1s Bloch wave has electron density strongly localised to the nuclei; this is the Bloch wave strongly scattered by TDS!
- TDS: inelastic but energy transfer small (e.g. ~0.015 eV): quasi-elastic. Essentially incoherent scattering ⟹ incoherent imaging
- However momentum transfer large ⟹ scattering to large ang (i.e. to HAADF detector)
- Indeed TDS intensity becomes greater than elastic scattering intensity for large scattering angles
- Most column simulation: *Frozen Phonon/Frozen Lattice*
  - Electrons faster than phonon vibrations ⟹ each electron "sees" static crystal lattice of displaced atoms
  - Propagate electron wave across different configurations of static lattices where atoms displaced according e.g. according to Einstein model
  - Propagation by multi-slice method: electron wave propagated across slices of differently displaced atoms

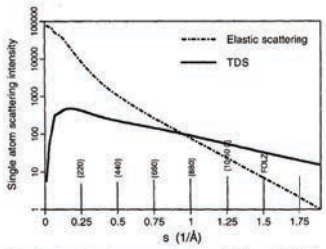

Figure 2. Theoretically calculated atom scattering factor $|(f^e)^2 \exp(-2W)|$ for elastic scattering and atom scattering factor $(f^e)^2[1-\exp(-2W)]$ for the TDS of a Si atom, showing the dominant contribution of TDS at large scattering angles, where W is the Debye–Waller factor. The scattering vector $\mathbf{s} = \mathbf{g}/2$. The rms atomic vibration amplitude was taken as 0.07 Å in the calculation.

Z.L. Wang Phil. Mag. B 79 (1999) 37–48;
Z.L. Wang *Elastic and Inelastic Scattering in Electron Diffraction and Imaging*, Plenum Press, p. 150–160

Other imaging modes

Medium-angle ADF (MAADF)

- Analysis of monolayer materials: low kV essential to prevent knock-on damage; here 60 kV used (knock-on threshold for bulk grapheme ~86 kV)
- As λ increases aberration correction even more important for obtaining atomic resolution
- Medium-angle ADF gives intensity $I \propto Z^{1.7}$ but with increased signal intensity compared to true HAADF image,; this intensity is needed for imaging single atom by single atom (here β = 58–200 mrad)

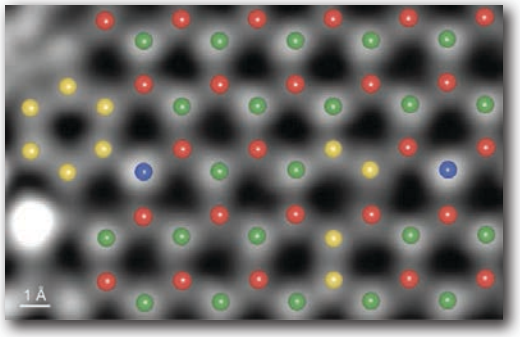

Krivanek et al Nature **464** (2010) 571

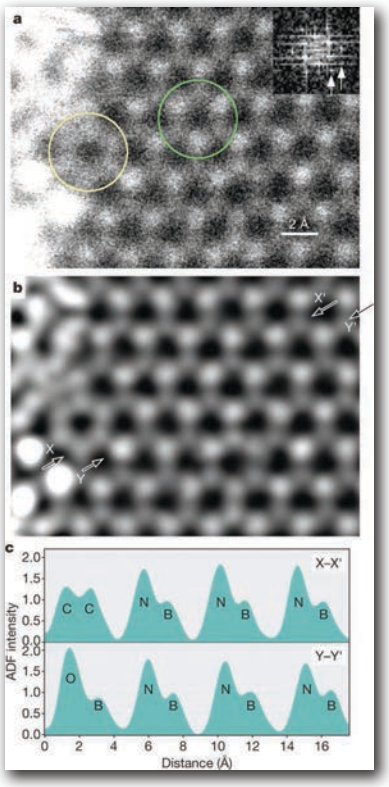

Annular bright-field (ABF) imaging

- HAADF not useful for imaging light atoms in a sample with heavy atoms because contrast so strongly dependent on atomic number
- BF imaging has same disadvantages for imaging light atom columns as phase-contrast HR-TEM imaging
- Annular bright-field imaging (with aberration correction), where central part of BF detector is obscured, apparently solves these problems. For instance, for α = 22 mrad, use β = 11–22 mrad.

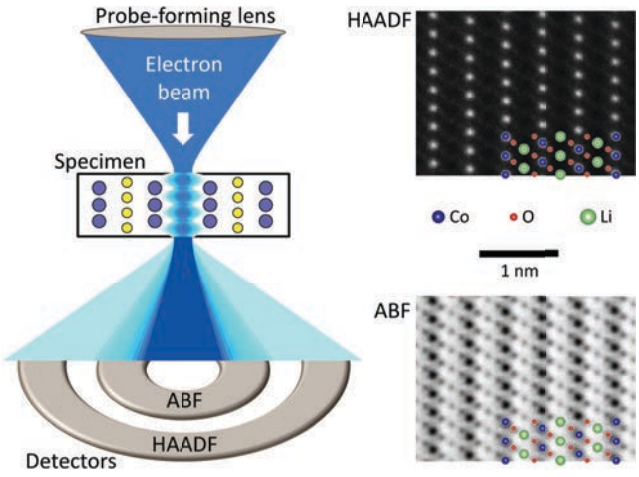

Direct visualization of lithium via annular bright field scanning transmission electron microscopy: a review
Findlay et al. Microscopy **66** (2017) 3–14
https://doi.org/10.1093/jmicro/dfw041

Annular bright-field (ABF) imaging

- Simulations show the ABF detector produces an "absorption" image in which light and heavy columns are visible and interpretable over a wide thickness range. Even H columns have been imaged.
- Simple theory: channeled electrons scattered mostly into centre of BF detector by light columns giving some dark ABF contrast; scattered more strongly to diffracted beams by heavy columns giving darker ABF contrast. Off column little scattering so brighter ABF contrast.
- Optimal focal range very small (like HAADF) but slightly different optimum defocus to HAADF.

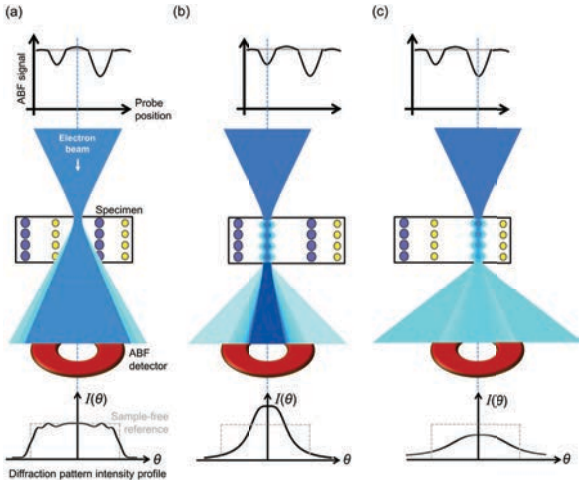

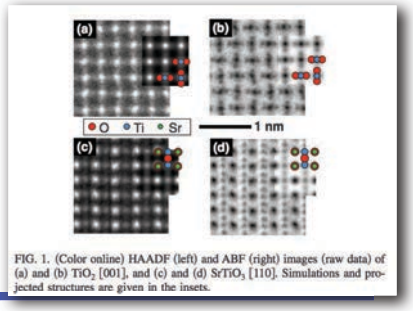

FIG. 1. (Color online) HAADF (left) and ABF (right) images (raw data) of (a) and (b) TiO_2 [001], and (c) and (d) $SrTiO_3$ [110]. Simulations and projected structures are given in the insets.

Findlay et al. APL **95** (2009) 191913

Differential Phase Contrast (DPC) imaging

- Use segmented detector illuminated by the direct (0 0 0) disc
- Measure intensity difference between two opposing quadrants
- For weakly scattering objects this represents gradient of the object potential (i.e. object electromagnetic field)

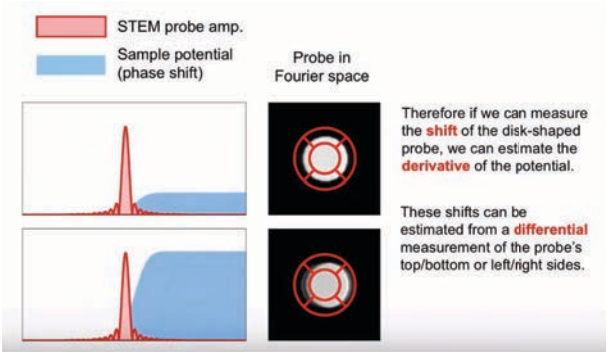

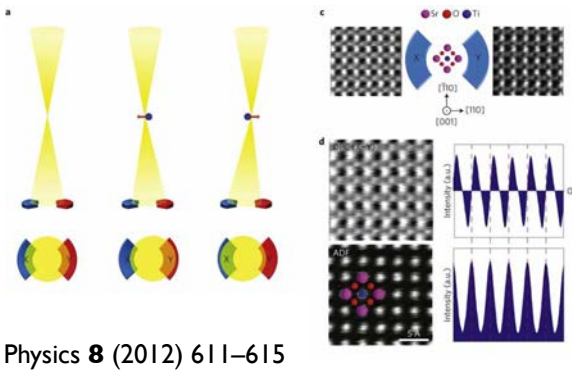

Shibata et al. Nature Physics **8** (2012) 611–615

Integrated Differential Phase Contrast

- Again use segmented detector illuminated by the direct (0 0 0) disc
- Calculate displacements of the centre of mass of this disc in function of probe position
- Displacement scales ~linearly with atomic number Z
  => atomic imaging for atoms from light to heavy
- Inherently phase contrast technique: analogous to calculation of mean inner potential by exit wave reconstruction of HRTEM?

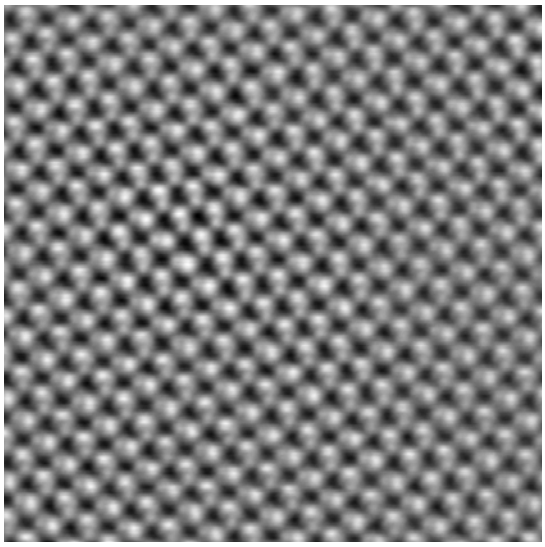

ZnO on [1 0 0 zone axis]

Lazic et al Ultramicroscopy **160** (2016) 265

Integrated Differential Phase Contrast

- Again use segmented detector illuminated by the direct (0 0 0) disc
- Calculate displacements of the centre of mass of this disc in function of probe position
- Displacement scales ~linearly with atomic number Z
  => atomic imaging for atoms from light to heavy
- Inherently phase contrast technique: analogous to calculation of mean inner potential by exit wave reconstruction of HRTEM?

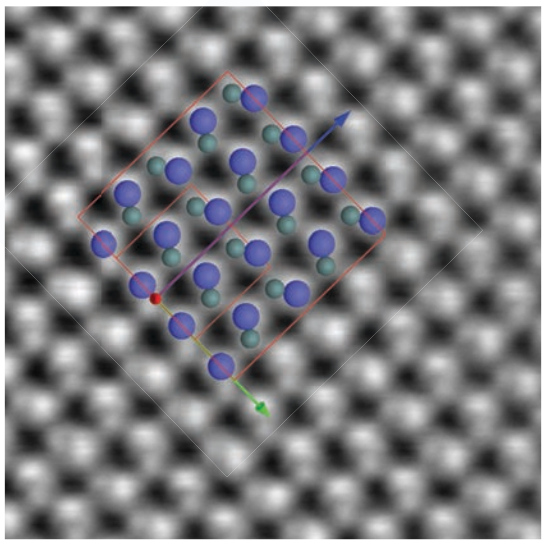

ZnO on [1 0 0 zone axis]

Lazic et al Ultramicroscopy **160** (2016) 265

4D STEM

- Differential phase contrast images can be made with 4 quadrant segmented detectors
- What if use 2D grid detector to record whole STEM CBED pattern? This is sometimes called "4D STEM"
- Currently very active area of EM research, with new detectors on market and developing applications
- Very rich (and large!) data sets, see this for some applications: https://www.youtube.com/watch?v=-KpxeNDoB5I

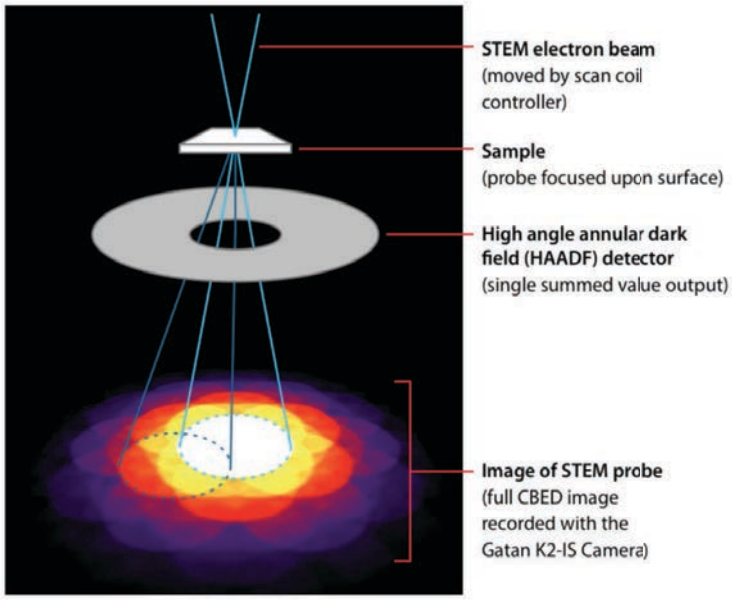

Schematic by Colin Ophus, Molecular Foundry

Limitations of STEM; references

- STEM (especially aberration-corrected) is powerful technique, but need:
  - Sample and stage stability, resistance to beam
  - Electronic stability in power supplies (no scan drift and/or distortion)
  - Minimum possible sample contamination
- These requirements are arguably more stringent than for TEM because of time needed to record a scan, and different type of beam dose and beam contamination (contamination mostly forms around the edge of a beam)
- References:
  - Stephen Pennycook "Scanning transmission electron microscopy : imaging and analysis" – *on-line for EPFL*
  - P. D. Nellist "Scanning Transmission Electron Microscopy", in *Science of Microscopy Vol. I* (ed. Stephen Hawkes) Springer 2007